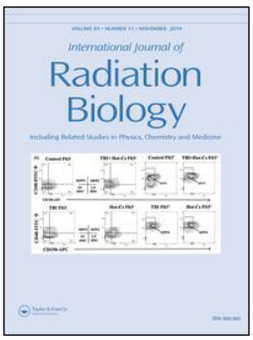

International Journal of Radiation Biology

ISSN: 0955-3002 (Print) 1362-3095 (Online) Journal homepage: https://www.tandfonline.com/loi/irab20

Coadministration of auraptene and radiotherapy; a novel modality against colon carcinoma cells *in vitro* and *in vivo*

Hamide Salari, Amin Afkhami-Poostchi, Shokouhozaman Soleymanifard, Saeideh Nakhaei-Rad, Elahe Merajifar, Mehrdad Iranshahi, Maryam M. Matin & Fatemeh B. Rassouli

To cite this article: Hamide Salari, Amin Afkhami-Poostchi, Shokouhozaman Soleymanifard, Saeideh Nakhaei-Rad, Elahe Merajifar, Mehrdad Iranshahi, Maryam M. Matin & Fatemeh B. Rassouli (2020): Coadministration of auraptene and radiotherapy; a novel modality against colon carcinoma cells *in vitro* and *in vivo*, International Journal of Radiation Biology, DOI: 10.1080/09553002.2020.1770359

To link to this article: https://doi.org/10.1080/09553002.2020.1770359

Accepted author version posted online: 15 May 2020.
Published online: 29 May 2020.

INTERNATIONAL JOURNAL OF RADIATION BIOLOGY
https://doi.org/10.1080/09553002.2020.1770359

Taylor & Francis
Taylor & Francis Group

ORIGINAL ARTICLE

Coadministration of auraptene and radiotherapy; a novel modality against colon carcinoma cells *in vitro* and *in vivo*

Hamide Salari[a]*, Amin Afkhami-Poostchi[a]*, Shokouhozaman Soleymanifard[b], Saeideh Nakhaei-Rad[c], Elahe Merajifar[a], Mehrdad Iranshahi[d], Maryam M. Matin[a,e,f], and Fatemeh B. Rassouli[e]

[a]Department of Biology, Faculty of Science, Ferdowsi University of Mashhad, Mashhad, Iran; [b]Medical Physics Research Center, Mashhad University of Medical Sciences, Mashhad, Iran; [c]Stem Cell Biology and Regenerative Medicine Research Group, Institute of Biotechnology, Ferdowsi University of Mashhad, Mashhad, Iran; [d]Biotechnology Research Center, Pharmaceutical Technology Institute, Mashhad University of Medical Sciences, Mashhad, Iran; [e]Novel Diagnostics and Therapeutics Research Group, Institute of Biotechnology, Ferdowsi University of Mashhad, Mashhad, Iran; [f]Stem Cells and Regenerative Medicine Research Group, Iranian Academic Center for Education, Culture and Research (ACECR), Khorasan Razavi, Mashhad, Iran

ABSTRACT

Background: Use of ionizing radiation (IR) is a common therapeutic modality for patients with colon carcinoma, although resistance of cancer cells and unintended toxicity reduce clinical outcomes.

Purpose: To enhance radioresponse of colon cancer cells, we designed a novel approach using auraptene (AUR) in combination with ionizing radiation (IR).

Methods: For in vitro studies, CT26 cells were pretreated with AUR and irradiated at different doses. Then, cell viability was evaluated by alamarBlue assay, and the mechanism of cell death was elucidated using annexin V-PI. To determine efficacy of our combined therapeutic modality in vivo, AUR was injected intraperitoneally to murine models of colon carcinoma followed by IR, and then quantitative measurements and histopathological examinations were performed. For molecular analyses, real time PCR and Western blot were carried out.

Results: Assessment of cell viability indicated significant enhancement of IR effects by AUR that was also confirmed by increased number of apoptotic cells. In vivo studies further demonstrated improved outcome in IR, since significant regression in tumor size was observed after administration of AUR + IR. Molecular analyses revealed down regulation of *Cyclin D1* and *CD44*, along with involvement of PI3K-AKT-mTORC signaling pathway and Caspase-3 in observed combinatorial effects.

Conclusion: Taken together, current findings support our previous reports on sensitizing effects of AUR and that AUR could be used as a promising adjunct to IR in cancer treatment.

Abbreviations: AKT: protein kinase B; AUR: auraptene; CRC: colorectal cancer; DMEM: Dulbecco's modified Eagle's medium; DMSO: dimethyl sulfoxide; FBS: fetal bovine serum; FITC: fluorescein isothiocyanate; IR: ionizing radiation; mTOR: mammalian target of rapamycin; NMR: nuclear magnetic resonance; PI: propidium iodide; PI3K: phosphatidylinositol-3-kinase; RPMI: Roswell Park Memorial Institute; real time PCR: real time polymerase chain reaction; SDS-PAGE: sodium dodecyl sulfate polyacrylamide gel electrophoresis

ARTICLE HISTORY
Received 20 October 2019
Revised 5 March 2020
Accepted 4 May 2020

KEYWORDS
Auraptene; Ionizing radiation; radiosensitizer colon carcinoma; combinatorial approach

1. Introduction

Recent reports on global burden of cancer have indicated that colorectal cancer (CRC) is the third common diagnosed malignancy, which ranks second in term of mortality (Bray et al. 2018; Ferlay et al. 2019). Although growing incidence of CRC has been associated with dietary habits, obesity and lifestyle factors, declined mortality rate in more developed countries reflects advancements in cancer diagnosis and treatment (Arnold et al. 2017). Multimodal therapeutic approaches that include ionizing radiation (IR) are used in adjuvant treatment of CRC to reduce local failure and distant metastasis (Hafner and Debus 2016). Coadministration of classical chemotherapeutic agents with IR has improved survival of CRC patients, however, unintended toxic effects on normal tissues, as well as intrinsic or acquired resistance of cancer cells, have prompted the investigations on specific agents as radiosensitizers (Bertocchi et al. 2016).

Prenyloxycoumarins are biosynthetic intermediates of coumarin derivatives, among which 7-geranyloxycoumarin, best known as auraptene (AUR), is the most abundant naturally occurring metabolite with numerous pharmacological

CONTACT Maryam M. Matin matin@um.ac.ir; Fatemeh B. Rassouli behnam3260@um.ac.ir Department of Biology, Faculty of Science, Ferdowsi University of Mashhad, Mashhad, Iran; Novel Diagnostics and Therapeutics Research Group, Institute of Biotechnology, Ferdowsi University of Mashhad, Mashhad, Iran
*Both authors have contributed equally to this work.

properties. In case of gastrointestinal cancers, valuable chemopreventive activity of AUR on rodent models of tongue, esophagus and colon cancers (Tanaka et al. 1998; Kawabata et al. 2000; Hayashi et al. 2007), as well as its growth inhibitory effects on human gastric and colon carcinoma cells (Epifano et al. 2013; Moon et al. 2015) have been determined. In addition, our previous reports indicated that AUR has the potential to improve efficacy of different anticancer modalities, including chemotherapy, IR and thermal therapy on esophageal and colon cancer cells (Saboor-Maleki et al. 2017; Moussavi et al. 2017, 2018).

Many investigations are currently focused on administration of compounds that could enhance sensitivity of cancer cells to conventional strategies, with minimal unfavorable effects on non-neoplastic cells. Since IR is used for palliation of CRC patients both at the site of primary tumor or metastatic lesions (Cameron et al. 2016), improving radiosensitivity of cancer cells would culminate in better clinical outcomes. Hence, we innovated a combined therapeutic modality against CRC based on AUR as a radiosensitizer agent. Accordingly, viability of mouse colon carcinoma cells was determined upon treatment with AUR and different doses of IR by alamarBlue assay, and induced apoptosis was detected by annexin V-PI flow cytometrically. For in vivo studies, AUR was injected intraperitoneally followed by IR exposure, and then, quantitative measurements and histopathological examinations were carried out. Finally, to have a better understating of AUR + IR mechanism of action, the expression of *Cyclin D1* and *CD44* were analyzed, and activation of PI3K-AKT-mTORC signaling pathway and also the amount of uncleaved Caspase-3 were studied by immunoblotting.

2. Materials and methods

2.2. Preparation of AUR

AUR was synthesized through a reaction between 7-hydroxycoumarin (1 M) and transgeranyl bromide (1.5 M) as described before (Askari et al. 2009). Column chromatography (petroleum ether/ethyl acetate 9:1 v/v) was performed for AUR purification (mp = 62.7–63.4 ꞉C), and ^{1}H- and ^{13}C-NMR experiments were used to confirm AUR structure. Different concentrations of AUR were prepared by dissolving 2 mg of white crystals in 100 µl dimethyl sulfoxide (DMSO, Merck), and then diluted by complete culture medium immediately before each experiment. For accurate interpretation of results, equal amounts of DMSO in all AUR concentrations (0.4% v/v) were considered as controls for in vitro experiments. Similarly, control groups for in vivo studies (DMSO and DMSO + IR) received 100 µl DMSO by intraperitoneal injection.

2.3. Treatment and viability assessment of cells

Cell lines used in current study were obtained from Pasteur Institute (Tehran, Iran). CT26 cells were grown in RPMI-1640 (Biowest) medium supplemented with 10% FBS (Biowest), while NIH/3T3 cells were cultured using Dulbecco's modified Eagle's medium (DMEM) containing 10% FBS. Cells were incubated at 37 °C in a humidified atmosphere of 5% CO_2 in air, and subcultured by 0.25% trypsin-1 mM EDTA (Biowest) as required.

To evaluate viability of cells upon single administration of AUR, CT26 and NIH/3T3 cells (2000 and 8000 cells in each well of 96 well plate, respectively) were treated with 5, 10 and 15 µg/ml AUR for 5 consecutive days. By the end of each time point, alamarBlue reagent (Sigma) was added (20 µl/well) and cells were incubated at 37 °C up to 90 min. Finally, absorbance was measured at 600 nm using a microplate reader (Epoch) and cell viability (%) was calculated by the following formula: 100-(AT-AU)/(AB-AU), in which AT, AU and AB are absorbance of treated cells, untreated cells and blank control, respectively.

In combinatorial treatments, CT26 cells were first treated with AUR for 24, 48 and 72 h. Afterwards, cells were exposed to IR using an X-ray linear accelerator (Philips, dose rate: 151.106 cGy/min) at three different doses (2, 4 and 6 Gy). Then, cells were recovered for 48 and 72 h at 37 °C, and finally, they were assessed for viability.

2.4. Detection of apoptosis

Upon combinatorial treatments of CT26 cells, apoptosis was assessed by fluorescein isothiocyanate (FITC) annexin V and propidium iodide (PI, BioLegend) according to the manufacturer's protocol. Briefly, treated cells and their relevant controls were collected, suspended in staining buffer, and stained with FITC-annexin V and PI for 15 min at room temperature in the dark. Finally, binding buffer was added, and cells were analyzed by flow cytometry (BD-Accuri C6) using FL1 and FL2 filters.

2.5. Tumor implantation and treatments

BALB/c male and female mice were maintained and reproduced in an animal house at Ferdowsi University of Mashhad (FUM) and experiments were carried out on their male offspring (6–8 weeks of age). Mice were provided with water and laboratory chow and housed at 25 ± 2 °C and a 12 h light-dark cycle, and all experiments were conducted in accordance with FUM approved codes of the care and use of laboratory animals.

Mice were subcutaneously implanted with CT26 cells (2×10^6 cells/100 µl PBS) in the right flank, and implanted tumors were allowed to reach the volume of 100-300 mm^3. Then, animals were randomly divided into six groups; PBS group ($n = 4$) received intraperitoneal (i.p.) injection of 100 µl PBS for 3 consecutive days, DMSO group ($n = 4$) received DMSO in the same manner and AUR group ($n = 5$) received i.p. injection of 100 mg/kg AUR for 3 days. For the next three groups, combinatorial approaches were performed in the same way, as PBS + IR group ($n = 6$) received i.p. injection of 100 µl PBS during 3 consecutive days, and on day 3, animals were exposed to 10 Gy local IR using X-ray linear accelerator, DMSO + IR group ($n = 6$)

received i.p. injection of 100 µl DMSO for 3 days followed by 10 Gy local IR exposure, and AUR + IR group ($n = 8$) received i.p. injection of 100 mg/kg AUR for 3 days followed by exposure to 10 Gy local IR. To note, mice in these three groups were anesthetized for 10 min with combination of ketamine and xylazine (Alfasan) before IR exposure.

During 10 days post-radiation, tumor volume (length × width × height × 0.5) was measured by a single observer with a digital caliper (Mitutoyo) with 0.01 mm precision. Relative tumor volume (RTV) was calculated as follows: V/V_0, where V and V_0 were mean TV of each group at a given time and at the beginning of measurements, respectively (Wang et al. 2015). In addition, to calculate tumor growth inhibition (TGI), the following formula was used: $(V/V_0)/(V_k/V_{k0}) \times 100$ where V_k and V_{ko} were mean TV of control group at a given time and at the beginning of measurement, respectively (Brezaniova et al. 2016). Finally, all mice were sacrificed, fresh tumor tissues were collected for molecular analysis, while the rest of tumor as well as spleen and liver of each animal were fixed and used for histopathological examinations upon hematoxylin and eosin staining.

2.6. Gene expression analysis

To analyze the expression of *Cyclin D1* and *CD44* upon combinatorial treatment, total RNA was extracted from all experimental groups using an RNA isolation kit (Riz Molecule DANA). Then, cDNA was synthesized using M-MuLV reverse transcriptase (Takara) according to the manufacturer's instruction, and fidelity of amplified cDNAs was confirmed by PCR using *β-Actin* primers (F: CGCCA CCAGTTCGCCATGGA and R: TACAGCCCGG GGAGCATCGT). Real time PCR was conducted in iQ5 real time PCR detection system (Bio-Rad) using SYBR green mix (Amplicon) and specific primers for *Cyclin D1* (F: AGTGCGTGCAGAAGGAGATT and R: CACAACTTCTC GGCAGTCAA) and *CD44* (F: TGAAACATGCAG GTATGGGT R: GCTGAGGCATTGAAGCAATA). For data analysis, GenEx software was used and *β-Actin* transcripts were considered as internal control. PCR cycling conditions were as follow: 95 °C for 5 min, [95 °C for 15 s, 55 °C for 15 s, 72 °C for 15 s] (50 cycles) for *Cyclin D*1 and 95 °C for 5 min, [95 °C for 20 s, 60 °C for 30 s, 72 °C for 30 s] (40 cycles) for *CD44*.

2.7. Western blot analysis

For total protein extraction, cells treated with AUR and IR alone or in combination, as well as their relevant DMSO controls, were harvested in lysis buffer (50 mM Tris-HCl pH 7.5; 100 mM NaCl, 2 mM $MgCl_2$; 1% triton X-100; 10% glycerol; 20 mM beta-glycerophosphate; 1 mM Ortho-Na_3VO_4; and EDTA-free protease inhibitor (Roche, Germany)). After determining protein concentration with Bradford assay, a total of 30 µg protein was separated by 10% (w/v) sodium dodecyl sulfate polyacrylamide gel electrophoresis (SDS-PAGE). The protein bands were then electroblotted onto a nitrocellulose membrane (Amersham Protran) and blocked in TBST buffer (Tris-buffered saline, 0.05% Tween 20; Sigma) containing 5% nonfat milk (Bio-Rad) for 1 h. Afterwards, proteins were incubated overnight at 4 °C with primary antibodies diluted in 5% nonfat milk/TBST: mouse anti-γ-tubulin (Sigma-Aldrich, #T5326), anti-rabbit Cyclin D1 (Cell Signaling, #55506), anti-rabbit phospho-AKT (S473, Cell Signaling, #4060), anti-rabbit AKT (Cell Signaling, #4691) and anti-rabbit Caspase-3 (Cell Signaling, #14220) and followed by incubation with peroxidase-conjugated anti-mouse/rabbit IgG (Cell Signaling) at room temperature for 1 h. Then, blots were developed using enhanced chemiluminescence (Clarity Western ECL Substrate, Bio-Rad) and detected by a bioimaging system (G-Box syngene). The density of each band was quantified by densitometry of scanned signals with the aid of Image Studio (version 5.2). For Cyclin D1 blotting, the obtained densitometry values for each condition in all groups were normalized to γ-tubulin and divided to PBS control. For pAKT blot, density of each band was normalized to the total amount of AKT (pAKT/AKT) and within individual groups (−IR and +IR) was divided separately to their PBS controls.

2.8. Statistical analyses

Normal distribution of data was determined by Kolmogorov-Smirnov normality test followed by one-way ANOVA or Mann-Whitney nonparametric analysis using SPSS software. Values were expressed as mean ± SEM, and p values less than .05 and .01 were considered to be statistically significant.

3. Results

Viability assessment of CT26 and NIH/3T3 cells indicated low toxicity of AUR during 5 days of treatments. Upon 120 h treatment with 10 and 15 µg/ml AUR, CT26 cell viability was calculated as 93% and 86%, respectively, and these data were determined as 85% and 73% for NIH/3T3 cells, respectively. Noticeably, viability of both cell types was higher in shorter periods (data not shown).

As shown in Figure 1, pretreatment of CT26 cells with AUR followed by IR exposure at different doses resulted in enhanced radioresponse of cells. Most notably, 10 and 15 µg/ml AUR increased toxicity of 4 Gy IR up to 15.6% and 31.2% after 48 h recovery time (Figure 1(B)) and up to 28.3% and 32% when cells were recovered for 72 h (Figure 1(E)). In addition, improved efficacy of 6 Gy IR by 10 and 15 µg/ml AUR were calculated as 19.5% and 29.4% after 48 h recovery of cells (Figure 1(C)). Further evaluating AUR effects on IR-induced cell death by flow cytometry revealed considerable increase in the percentage of early and late apoptotic cells (Figure 2(A)). Likewise, morphological alterations, in the form of dispersed cells with cytoplasmic granulation, were obvious after coadministration of AUR and IR in comparison with control treatments (Figure 2(B–E)).

Role of AUR as a radiosensitizer in vivo was also examined in BALB/c mice bearing CT26 colon carcinoma. After three consecutive injections with PBS, DMSO or AUR

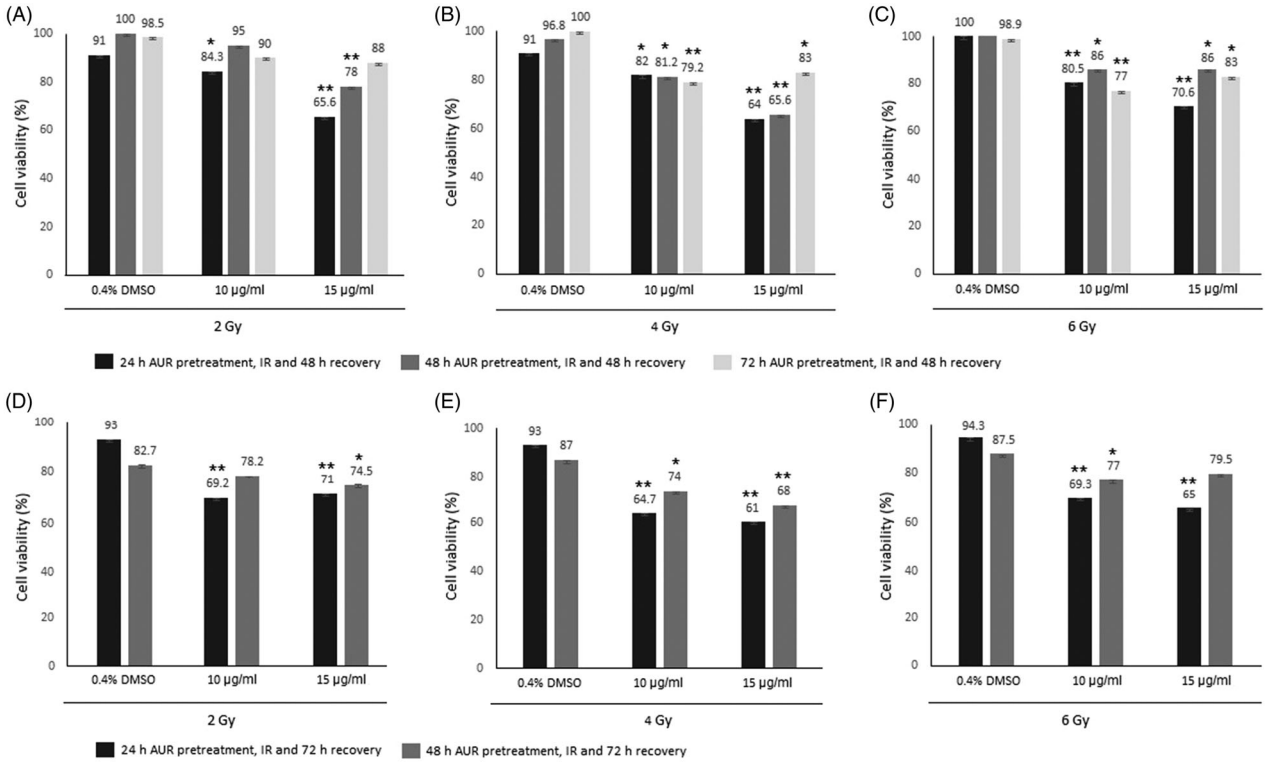

Figure 1. Viability assessment of CT26 cells upon combinatorial treatment with AUR + IR. After pretreatment of cells with AUR, IR was applied at 2 Gy (A and D), 4 Gy (B and E) and 6 Gy (C and F), and cells were recovered for 48 h (A–C) or 72 h (D–F). $^{*}p < .05$, $^{**}p < .01$, indicate significant difference with relevant control (0.4% DMSO + IR with similar dose and recovery time). Viability assessment was carried out for at least three times and results are presented as mean ± SEM.

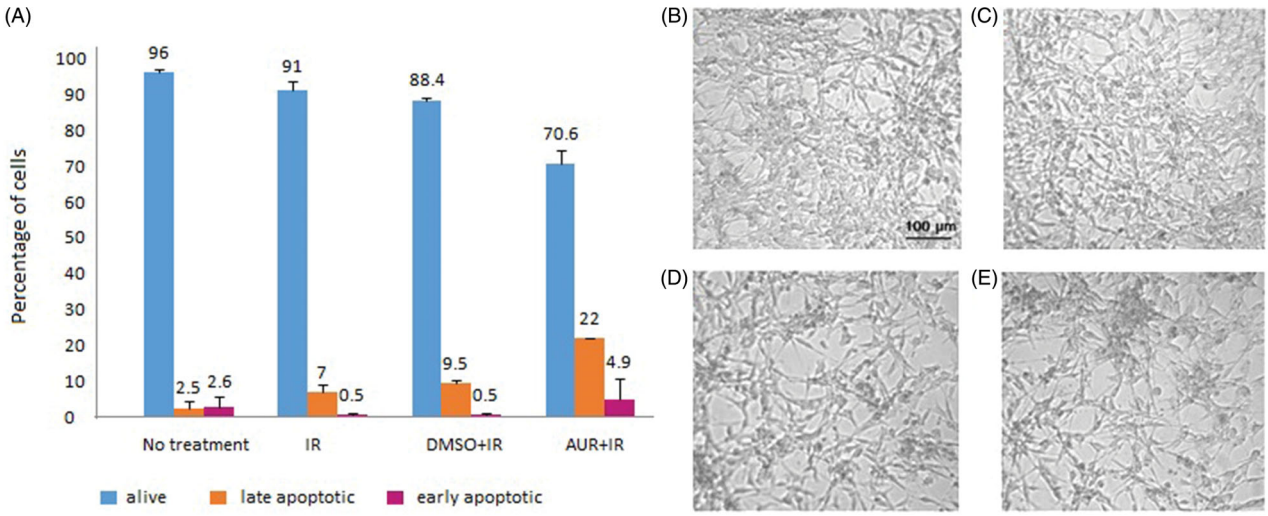

Figure 2. Apoptosis detection and morphological alterations in CT26 cells. Flow cytometric detection of alive, necrotic and apoptotic cells after different treatments, which are presented as mean ± SEM (A). Phase contrast photomicrographs of cells exposed to 4 Gy radiation (B), pretreated with 0.4% DMSO (C), 10 μg/ml (D) or 15 μg/ml (E) AUR followed by 4 Gy IR with 72 h recovery time.

(100 mg/kg bw), three groups received localized IR (10 Gy) and all animals were examined for tumor growth during 10 days. As shown in Figure 3(A,B), absolute tumor volumes in all groups except AUR + IR increased in a time-dependent manner. At the end of experiment (day 10), RTVs of PBS + IR, DMSO + IR and AUR + IR groups were 5.2 ± 2.7, 7.3 ± 3.06 and 0.12 ± 0.05, respectively, all significantly ($p < .01$) smaller than that of DMSO group (36.7 ± 5.02). To note, RTV in AUR group (16.5 ± 5.28) was also significantly ($p < .05$) smaller than that in DMSO group (Figure 3(C)). To have a better evaluation of treatments efficacy, TGI was also calculated. Figure 3(D) demonstrates TGI of each combinatorial approach based on its relevant single treatment. On day 10, TGI was 99% for AUR + IR group, significantly ($p < .01$) higher than that for PBS + IR and DMSO + IR groups (73% and 81%, respectively). In addition, when TGI

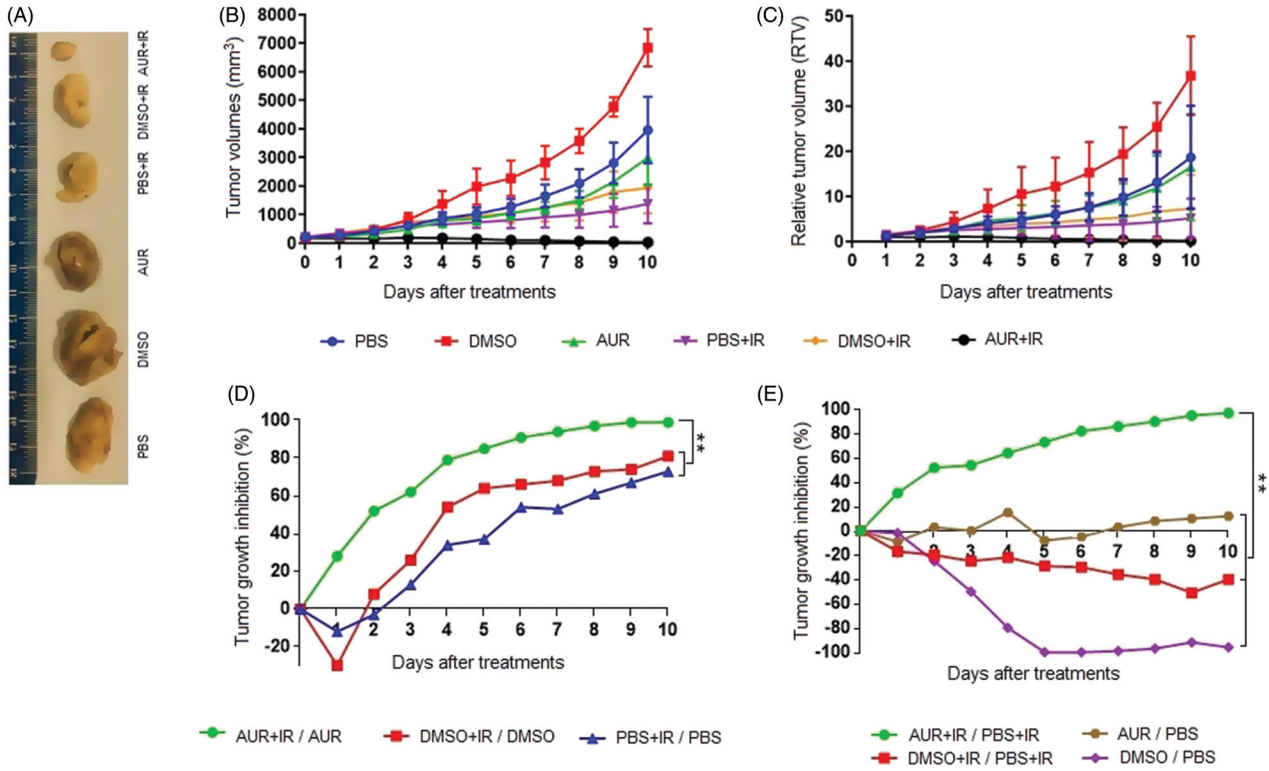

Figure 3. Effects of various treatments on tumor growth. Representative image of tumor size following different treatments (A). The absolute tumor volumes (B) and relative tumor volumes (RTV, C) during 10 days post-radiation in six groups. Depiction of TGI in animals receiving PBS, DMSO or AUR followed by IR based on single use of each agent (D). Calculated TGI in animals receiving AUR and DMSO alone or in combination with IR based on relevant PBS controls (E). $^{**}p < .01$, indicates significant difference between groups. The number of animals in different groups were as follows: $n = 4$, $n = 3$ and $n = 5$ in PBS, DMSO and AUR groups, respectively, and $n = 6$ in each of the PBS + IR, DMSO + IR and AUR + IR groups.

of AUR alone or + IR was calculated based on their relevant PBS controls (Figure 3(E)), a significant ($p < .01$) higher inhibitory effect of combinatorial approach was indicated again (12% *vs* 97%, respectively). Accordingly, injection of AUR followed by IR resulted in a substantial growth delay and subsequent inhibition of tumor growth rate, mainly due to increased susceptibility of cancer cells to IR. Nevertheless, DMSO injection, alone or followed by IR, had promoting effects on tumor growth.

In accordance with quantitative measurements of tumors, histopathological examinations revealed increased number of apoptotic cells only in tumor tissues of AUR + IR group (Figure 4(A–F)). Although one mouse in DMSO and two mice in AUR + IR groups died during the study, evaluating toxicity of our combinatorial approach by assessment of spleen and liver revealed normal tissue microstructures in all experimental groups (Figure 4(G–R)), similar to the mean body weights in all groups that were not significantly different at the beginning and end of the experiments (data not shown).

To have a better understating of AUR + IR effects and elucidate its mechanism of action, tumor tissues were analyzed for the expression of candidate genes by real time RT-PCR (Figure 5(A)). Accordingly, down regulation of *Cyclin D1* was observed in PBS + IR and AUR + IR groups (−1.8 and −3, respectively), while it was only significant ($p < .01$) in AUR + IR group. Moreover, reduced expression of *CD44* was observed in PBS + IR and AUR + IR groups (−1.1 and −0.6, respectively), although not significant. As illustrated in Figure 5(B), the amount of Cyclin D1 was also evaluated at translational level, and results showed reduced amount of Cyclin D1 upon IR administration. More specifically, Cyclin D1 expression was lower in AUR + IR in comparison with its relevant control, DMSO + IR. In addition, the impact of AUR + IR treatment was elucidated on PI3K-AKT-mTORC signaling pathway that is one of the main pathways regulating cell survival (Figure 5(C)). Applying antibody against phosphorylated AKT at position Ser-473, which is downstream of mTOR kinase, in immunoblotting analysis indicated that IR alone increased pAKT to AKT ratio (PBS+IR), although coadministration of AUR + IR prevented activation of AKT pathway. Finally, to determine whether AUR + IR induces apoptosis, we checked the amount of uncleaved Caspase-3 protein in all groups (Figure 5(C)), and interestingly, reduced amount of uncleaved Caspase-3 was only detected in AUR + IR, probably due to its cleavage and subsequent activation.

4. Discussion

Radiotherapeutic modalities are indispensible for management of CRC, especially when patients struggle with local relapse or oligometastases (Hafner and Debus 2016). With the hope to improve clinical outcomes, use of agents that could enhance radioresponse of cancer cells while having nonoverlapping toxicities is an area of evolving interest. AUR is a natural prenyloxycoumarin with considerable pharmacological properties, such as chemopreventive and

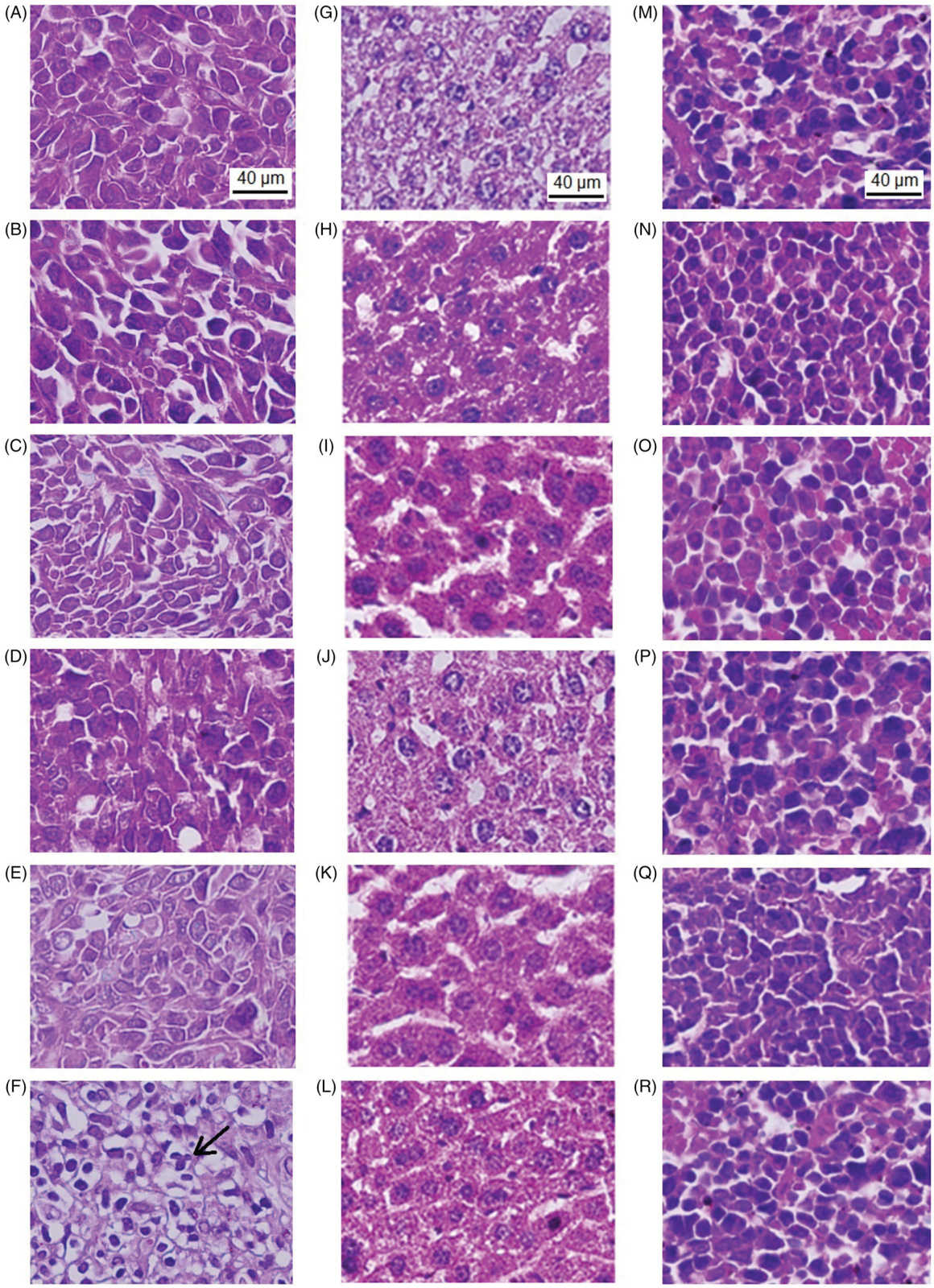

Figure 4. Photomicrographs of tumor (A–F), liver (G–L) and spleen (M–R) cross sections in six groups; PBS (A, G and M), DMSO (B, H and N), AUR (C, I and O), PBS + IR (D, J and P), DMSO + IR (E, K and Q) and AUR + IR (F, L and R). Apoptotic cells with vacuolated cytoplasm and condensed nuclei can be observed in tumor section of AUR + IR group (black arrow).

anticancer effects. To expand our previous findings on sensitizing effects of AUR (Saboor-Maleki et al. 2017; Moussavi et al. 2017, 2018), we innovated an approach against CRC based on combinatorial use of AUR and IR.

Although several reports have introduced AUR as an anticancer agent that acts through various mechanisms such as stimulation of caspase cascade or suppression of mTOR pathway (Moon et al. 2015; Lee et al. 2017), few studies

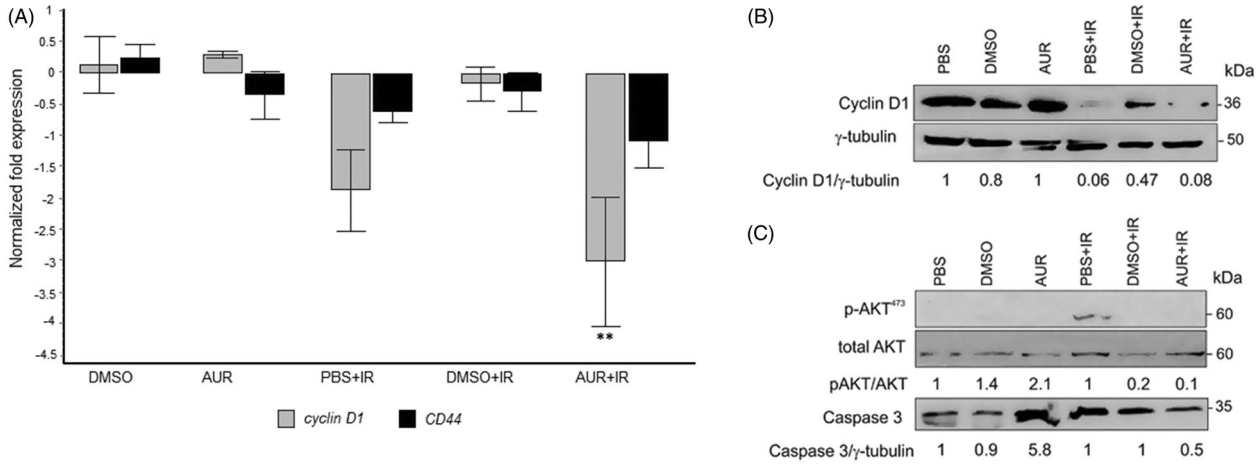

Figure 5. Expression pattern of *Cyclin D1* and *CD44* (A and B) and involvement of PI3K-AKT-mTORC pathway and Caspase-3 (C) in observed effects of AUR + IR treatment. Normalized values were plotted as relative fold-change compared with PBS group (A). $^{**}p < .01$ significant difference with PBS group. Cyclin D1 protein levels were detected with anti-Cyclin D1 antibody and normalized to the amount of γ-tubulin (B). Immunoblotting of the total AKT and phosphorylated AKT at position of Ser-473 (downstream of mTORC kinase), as well as the amount of uncleaved Caspase-3 (35 kDa) upon treatment with AUR alone or in combination with IR (C, data are representative of two unrelated experiments). Here, the numbers below blots indicate pAKT/AKT and Caspase 3/gamma-tubulin ratios within individual groups, −IR and +IR, where these amounts are separately normalized to their control PBS and PBS+IR, respectively. Total AKT and γ-tubulin served as controls.

have evaluated its effects in combination with other therapeutic modalities. In case of chemotherapy, synergy between AUR and anticancer drugs have been demonstrated in different cancer cell types (Nabekura et al. 2008; Kleiner-Hancock et al. 2010; Moussavi et al. 2017; Saboor-Maleki et al. 2017), as well as its improving effects on thermal therapy in colon carcinoma cells (Moussavi et al. 2018). Viability assessment of cells in present study revealed low toxicity of 10 µg/ml AUR on both normal and cancer cells, even after 5 days of treatments. Interestingly, when used in combination with IR, AUR significantly enhanced radioresponse of colon carcinoma cells and this finding was further confirmed by flow cytometry-based detection of apoptotic cells. Similarly, we have shown accumulation of a sub-G_1 phase population of human colon adenocarcinoma cells after treatment with nontoxic concentrations of AUR followed by IR exposure (Moussavi et al. 2017). Since intracellular accumulation and biotransformation of AUR to its main metabolite, umbelliferone, occurs in a time dependent manner in vitro (Murakami et al. 2000), it seems that 24 h pretreatment of cells with AUR, followed by IR and 72 h recovery was long enough for radiosensitizing effects of AUR to be observed.

To investigate whether our previous and current in vitro results can be expanded to animal models, we performed further experiments in BALB/c mice inoculated with colon carcinoma cells. Six groups of animals received same volume (100 µl) of PBS, DMSO or AUR for 3 days, and right afterwards, three groups were exposed to localized IR. Examination of tumor growth during 10 days follow up indicated significant growth inhibition in AUR + IR group in comparison with all other animals, and intriguingly, toxic effects of our combined modality was observed in tumor samples, but not in spleen and liver tissues.

As reported previously, topical application of AUR (40 nM/40 days) reduced tumor incidence in mouse skin through suppression of superoxide generation (Murakami et al. 1997), and when injected subcutaneously (100 µM/6 days), AUR inhibited progression of renal cell carcinoma by disrupting VEGF-induced angiogenesis and reforming energy metabolism (Jang et al. 2015). Nevertheless, dietary administration of AUR (200 mg/kg bw/4 days) did not effectively suppress tumor volume in xenograft models (Kleiner-Hancock et al. 2010). Herein, i.p. injection of AUR (100 mg/kg bw/3 days) had no significant effect on tumor volume in comparison with PBS group, although its effect was comparable with DMSO group. Precise evaluation of AUR activity in our study requires considered analysis of DMSO effects, as DMSO alone or in combination with IR promoted tumor growth rather than inducing tumor inhibitory effects. Similarly, Jang et al. reported tumor growth upon intratumoral injection of DMSO, when compared with AUR received animals (Jang et al. 2015). Both observations could be explained by the work of Elisia et al., who indicated inefficiency of DMSO at reducing tumor growth, since it blocked activation of mouse macrophages and reduced levels of pro-inflammatory cytokines, IFN-γ and G-CSF (Elisia et al. 2016). Clearly, more research must be done to define other mechanisms involved in observed effects of DMSO in vivo.

IR is clinically applied as single or multiple fractions. Despite same efficacy of both approaches, single fraction IR is more convenient, cost conscious, time efficient and importantly, has less acute toxicity (Hartsell et al. 2009; Howell et al. 2013). A number of studies have indicated radiosensitizing effects of natural compounds in BALB/c mice inoculated with CT26 cells. For instance, etoposide and caffeic acid phenethyl ester improved efficacy of fractionated IR in animal models of colon carcinoma (Chen et al. 2005; Liu et al. 2005). In addition, there are few reports on the role of coumarin derivatives in radiosensitization of cancer cells including osthole (Peng et al. 2018), a synthetic isocoumarin derivative (NM-3) and

metronidazole-coumarin conjugates (Salloum et al. 2000; Bonneau et al. 2013). Present attempt, however, is the first study demonstrating considerable effects of AUR as a natural coumarin that enhanced sensitivity of cancer cells to single fraction IR in vivo.

Molecular analysis revealed, to some extent, the underlying mechanisms of observed effects in vitro and in vivo, since coadministration of AUR and IR down regulated *Cyclin D1* and *CD44*, inhibited PI3K-AKT-mTORC signaling pathway and induced apoptosis via Caspase-3.

Agents that enhance IR sensitivity of cancer cells generally do so by inhibiting progression through cell cycle, DNA repair mechanisms and/or signaling cascades that regulate cell survival and apoptosis (Mierzwa et al. 2010). Meanwhile, inhibitory effects of AUR on cell proliferation were linked to down regulation of genes involved in cell cycle control such as *Cyclin D1* and *E2F1* (Krishnan and Kleiner-Hancock 2012), and self renewal including *CD44* and *BMI-1* (Moussavi et al. 2017; Saboor-Maleki et al. 2017). Molecular analysis of treated cells and tumor tissues in present study revealed significant down regulation of *Cyclin D1*, as well as reduced expression of *CD44,* in AUR + IR group. Accordingly, improved sensitization of colon cancer cells to IR by AUR can be partially due to their arrested cell cycle and inhibited proliferation.

Despite the fact that IR impedes growth of cancer cells by inducing cytotoxicity, it simultaneously induces a number of pro-survival and anti-apoptotic signaling pathways, like those mediated by AKT (Hein et al. 2014). Similar to another report on IR-induced activity of AKT in human colon carcinoma cells (Yacoub et al. 2006), our findings indicated increased AKT activity, as elucidated by pAKT (Ser-473), upon IR administration. Interestingly, combinatorial use of AUR + IR prevented phosphorylation of AKT downstream target, which also confirms reported role for AUR as an mTOR inhibitor (Moon et al. 2015).

Depending on the dose and tumor cell type, IR induces intrinsic or extrinsic apoptotic pathways (Maier et al. 2016), and upon activation of both pathways, Caspase-8 and Caspase-9 cleave and activate Caspase-3 (McArthur and Kile 2018). Our findings showed reduced amount of uncleaved Caspase-3 upon AUR + IR treatment that is probably due to cleavage and activation of this protein. Accordingly, inhibition of PI3K-AKT-mTORC signaling pathway and activation of Caspase-3 could be other mechanisms that explain observed effects of AUR + IR approach.

In conclusion, current findings confirm our previous reports on radiosensitizing effects of AUR. The fact that AUR improved radioresponse of murine colon carcinoma cells without toxicity in vivo suggests that it could be used as a promising adjunct to IR in cancer treatment. Nevertheless, more investigations are required to adopt AUR as a standard radiosensitizer in routine clinical practice.

Acknowledgements

The authors would like to thank Dr. Kamel, Dr. Norouz Pour and Mr. Mirahmadi for their help and technical advices.

Disclosure statement

The authors declare that they have no known competing financial interests or personal relationships that could have appeared to influence the work reported in this paper.

Funding

This work was supported with grants from Iran National Science Foundation [INSF, No. 95849744] and Ferdowsi University of Mashhad [No. 46686].

Notes on contributors

Hamide Salari, holds an M.Sc. in Cell and Molecular Biology from Ferdowsi University of Mashhad, and is currently investigating other biological effects of auraptene in vitro.

Amin Afkhami-Poostchi, is pursuing a PhD in Cell and Molecular Biology, Ferdowsi University of Mashhad, and studies anticancer effects of synthetic/natural compounds in vivo.

Shokouhozaman Soleymanifard, is an Assistant Professor of Medical Physics, Mashhad University of Medical Sciences, and does research in cancer therapy and medical physics.

Saeideh Nakhaei-Rad, is an Assistant Professor of Biochemistry, Ferdowsi University of Mashhad, and currently studies molecular mechanism of signaling networks in human cancers.

Elahe Merajifar, holds an M.Sc. in Cell and Molecular Biology from Ferdowsi University of Mashhad, and is currently investigating biological effects of natural compounds.

Mehrdad Iranshahi, is a Professor of Pharmacognosy, Mashhad University of Medical Sciences, and does tremendous research in cancer chemoprevention and therapy.

Maryam M. Matin, is a Professor of Molecular Biology, Ferdowsi University of Mashhad, and supervises outstanding projects in cancer diagnosis and therapy.

Fatemeh B. Rassouli, is an Assistant Professor of Cell and Molecular Biology, Ferdowsi University of Mashhad, and supervises research in cancer combinatorial therapy.

ORCID

Shokouhozaman Soleymanifard http://orcid.org/0000-0001-7417-989X
Mehrdad Iranshahi http://orcid.org/0000-0002-3018-5750
Maryam M. Matin http://orcid.org/0000-0002-7949-7712
Fatemeh B. Rassouli http://orcid.org/0000-0003-1889-0964

References

Arnold M, Sierra MS, Laversanne M, Soerjomataram I, Jemal A, Bray F. 2017. Global patterns and trends in colorectal cancer incidence and mortality. Gut. 66(4):683–691.

Askari M, Sahebkar A, Iranshahi M. 2009. Synthesis and purification of 7-prenyloxycoumarins and herniarin as bioactive natural coumarins. Iran J Basic Med Sci. 12:63–69.

Bertocchi P, Aroldi F, Prochilo T, Meriggi F, Beretta GD, Zaniboni A. 2016. Chemotherapy rechallenge after regorafenib treatment in metastatic colorectal cancer: still hope after the last hope. Chemother. 29:1–4.

Bonneau A, Maresca A, Winum JY, Supuran CT. 2013. Metronidazole-coumarin conjugates and 3-cyano-7-hydroxy-coumarin act as

isoform-selective carbonic anhydrase inhibitors. J Enzyme Inhib Med Chem. 28(2):397–401.
Bray F, Ferlay J, Soerjomataram I, Siegel RL, Torre LA, Jemal A. 2018. Global cancer statistics 2018: GLOBOCAN estimates of incidence and mortality worldwide for 36 cancers in 185 countries. CA Cancer J Clin. 68(6):394–424.
Brezaniova I, Hruby M, Kralova J, Kral V, Cernochova Z, Cernoch P, Slouf M, Kredatusova J, Stepanek P. 2016. Temoporfin-loaded 1-tetradecanol-based thermoresponsive solid lipid nanoparticles for photodynamic therapy. J Control Release. 241:34–44.
Cameron MG, Kersten C, Vistad I, Helvoirt RV, Weyde K, Undseth C, Mjaaland I, Skovlund E, Fossa SD, Guren MG. 2016. Palliative pelvic radiotherapy for symptomatic rectal cancer - a prospective multicenter study. Acta Oncol. 55(12):1400–1407.
Chen YJ, Liao HF, Tsai TH, Wang SY, Shiao MS. 2005. Caffeic acid phenethyl ester preferentially sensitizes CT26 colorectal adenocarcinoma to ionizing radiation without affecting bone marrow radioresponse. Int J Radiat Oncol Biol Phys. 63(4):1252–1261.
Elisia I, Nakamura H, Lam V, Hofs E, Cederberg R, Cait J, Hughes MR, Lee L, Jia W, Adomat HH, et al. 2016. DMSO represses inflammatory cytokine production from human blood cells and reduces autoimmune arthritis. PLoS One. 11(3):e0152538.
Epifano F, Genovese S, Miller R, Majumdar AP. 2013. Auraptene and its effects on the re-emergence of colon cancer stem cells. Phytother Res. 27(5):784–786.
Ferlay J, Colombet M, Soerjomataram I, Mathers C, Parkin DM, Piñeros M, Znaor A, Bray F. 2019. Estimating the global cancer incidence and mortality in 2018: GLOBOCAN sources and methods. Int J Cancer. 144(8):1941–1953.
Hafner MF, Debus J. 2016. Radiotherapy for colorectal cancer: current standards and future perspectives. Visc Med. 32(3):172–177.
Hartsell WF, Konski AA, Lo SS, Hayman JA. 2009. Single fraction radiotherapy for bone metastases: clinically effective, time efficient, cost conscious and still underutilized in the United States. Clin Oncol (R Coll Radiol). 21(9):652–654.
Hayashi K, Suzuki R, Miyamoto S, Shin-Ichiroh Y, Kohno H, Sugie S, Takashima S, Tanaka T. 2007. Citrus auraptene suppresses azoxymethane-induced colonic preneoplastic lesions in C57BL/KsJ-db/db mice. Nutr Cancer. 58(1):75–84.
Hein AL, Ouellette MM, Yan Y. 2014. Radiation-induced signaling pathways that promote cancer cell survival (review). Int J Oncol. 45(5):1813–1819.
Howell DD, James JL, Hartsell WF, Suntharalingam M, Machtay M, Suh JH, Demas WF, Sandler HM, Kachnic LA, Berk LB. 2013. Single-fraction radiotherapy versus multifraction radiotherapy for palliation of painful vertebral bone metastases-equivalent efficacy, less toxicity, more convenient: a subset analysis of Radiation Therapy Oncology Group trial 97-14. Cancer. 119(4):888–896.
Jang Y, Han J, Kim SJ, Kim J, Lee MJ, Jeong S, Ryu MJ, Seo K-S, Choi S-Y, Shong M, et al. 2015. Suppression of mitochondrial respiration with auraptene inhibits the progression of renal cell carcinoma: involvement of HIF-1α degradation. Oncotarget. 6(35):38127–38138.
Kawabata K, Tanaka T, Yamamoto T, Ushida J, Hara A, Murakami A, Koshimizu K, Ohigashi H, Stoner GD, Mori H. 2000. Suppression of N-nitrosomethylbenzylamine-induced rat esophageal tumorigenesis by dietary feeding of 1'-acetoxychavicol acetate. Cancer Res. 91(2):148–155.
Kleiner-Hancock HE, Shi R, Remeika A, Robbins D, Prince M, Gill JN, Syed Z, Adegboyega P, Mathis JM, Clifford JL. 2010. Effects of ATRA combined with citrus and ginger-derived compounds in human SCC xenografts. BMC Cancer. 10:394.
Krishnan P, Kleiner-Hancock H. 2012. Effects of auraptene on IGF-1 stimulated cell cycle progression in the human breast cancer cell line, MCF-7. Int J Breast Cancer. 2012:502092
Lee JC, Shin EA, Kim B, Kim BI, Chitsazian-Yazdi M, Iranshahi M, Kim SH. 2017. Auraptene induces apoptosis via myeloid cell leukemia 1-mediated activation of caspases in PC3 and DU145 prostate cancer cells. Phytother Res. 31(6):891–898.
Liu CY, Liao HF, Wang TE, Lin SC, Shih SC, Chang WH, Yang YC, Lin CC, Chen YJ. 2005. Etoposide sensitizes CT26 colorectal adenocarcinoma to radiation therapy in BALB/c mice. World J Gastroenterol. 11(31):4895–4898.
Maier P, Hartmann L, Wenz F, Herskind C. 2016. Cellular pathways in response to ionizing radiation and their targetability for tumor radiosensitization. IJMS. 17(1):102.
McArthur K, Kile BT. 2018. Apoptotic caspases: multiple or mistaken identities? Trends Cell Biol. 28(6):475–493.
Mierzwa ML, Nyati MK, Morgan MA, Lawrence TS. 2010. Recent advances in combined modality therapy. Oncologist. 15(4):372–381.
Moon JY, Kim H, Cho SK. 2015. Auraptene, a major compound of supercritical fluid extract of phalsak (Citrus HassakuHort ex Tanaka), induces apoptosis through the suppression of mTOR pathways in human gastric cancer SNU-1 cells. Evid-Based Compl Alt Med. 2015:1–10.
Moussavi M, Haddad F, Matin MM, Iranshahi M, Rassouli FB. 2018. Efficacy of hyperthermia in human colon adenocarcinoma cells is improved by auraptene. Biochem Cell Biol. 96(1):32–37.
Moussavi M, Haddad F, Rassouli FB, Iranshahi M, Soleymanifard S. 2017. Synergy between auraptene, ionizing radiation, and anticancer drugs in colon adenocarcinoma cells. Phytother Res. 31(9): 1369–1375.
Murakami A, Wada K, Ueda N, Sasaki K, Haga M, Kuki W, Takahashi Y, Yonei H, Koshimizu K, Ohigashi H. 2000. In vitro absorption and metabolism of a citrus chemopreventive agent, auraptene, and its modifying effects on xenobiotic enzyme activities in mouse livers. Nutr Cancer. 36(2):191–199.
Murakami A, Kuki W, Takahashi Y, Yonei H, Nakamura Y, Ohto Y, Ohigashi H, Koshimizu K. 1997. Auraptene, a citrus coumarin, inhibits 12-0-tetradecanoylphorbol-13-acetate-induced tumor promotion in ICR mouse skin, possibly through suppression of superoxide generation in leukocytes. Jpn J Cancer Res. 88(5): 443–452.
Nabekura T, Yamaki T, Kitagawa S. 2008. Effects of chemopreventive citrus phytochemicals on human P-glycoprotein and multidrug resistance protein 1. Eur J Pharmacol. 600(1–3):45–49.
Peng L, Huang YT, Chen J, Zhuang YX, Zhang F, Chen JY, Zhou L, Zhang DH. 2018. Osthole sensitizes with radiotherapy to suppress tumorigenesis of human nasopharyngeal carcinoma in vitro and in vivo. Cancer Manag Res. 10:5471–5477.
Saboor-Maleki S, Rassouli FB, Matin MM, Iranshahi M. 2017. Auraptene attenuates malignant properties of esophageal stem-like cancer cells. Technol Cancer Res Treat. 16(4):519–527.
Salloum RM1, Jaskowiak NT, Mauceri HJ, Seetharam S, Beckett MA, Koons AM, Hari DM, Gupta VK, Reimer C, Kalluri R, et al. 2000. NM-3, an isocoumarin, increases the antitumor effects of radiotherapy without toxicity. Cancer Res. 60(24):6958–6963.
Tanaka T, Kawabata K, Kakumoto M, Matsunaga K, Mori H, Murakami A, Kuki W, Takahashi Y, Yonei H, Satoh K, et al. 1998. Chemoprevention of 4-nitroquinoline 1-oxide-induced oral carcinogenesis by citrus auraptene in rats. Carcinogen. 19(3):425–431.
Wang L, Long L, Wang W, Liang Z. 2015. Resveratrol, a potential radiation sensitizer for glioma stem cells both in vitro and in vivo. J Pharmacol Sci. 129:216–225.
Yacoub A, Miller A, Caron RW, Qiao L, Curiel DA, Fisher PB, Hagan MP, Grant S, Dent P. 2006. Radiotherapy-induced signal transduction. Endocr Relat Cancer. 1:S99–S114.